

Identifying demographic and environmental drivers of population dynamics and viability in an endangered top predator using an integrated model

A. J. Warlick¹ , G. K. Himes Boor² , T. L. McGuire³ , K. E.W. Sheldon⁴ , E. K. Jacobson⁵ , C. Boyd¹ , P. R. Wade⁴ , A. E. Punt¹  & S. J. Converse⁶ 

¹ School of Aquatic and Fishery Sciences, University of Washington, Seattle, WA, USA

² Ecology Department, Montana State University, Bozeman, MT, USA

³ The Cook Inlet Beluga Whale Photo-ID Project, Anchorage, AK, USA

⁴ Marine Mammal Laboratory, Alaska Fisheries Science Center, NOAA, NMFS, Seattle, WA, USA

⁵ Center for Research into Ecological & Environmental Modelling, St Andrews, UK

⁶ U.S. Geological Survey, Washington Cooperative Fish and Wildlife Research Unit, School of Aquatic and Fishery Sciences & School of Environmental and Forest Sciences, University of Washington, Seattle, WA, USA

Keywords

Bayesian integrated population model; population viability analysis; Cook Inlet beluga whale; extinction risk; environmental variability; prey availability.

Correspondence

Amanda J. Warlick, School of Aquatic and Fishery Sciences, University of Washington, 1122 NE Boat St, Seattle, WA 98195, USA.
Email: awarlick@uw.edu

Editor: Rahel Sollmann

Associate Editor: Rob Williams

Received 21 October 2022; accepted 04 August 2023

doi:10.1111/acv.12905

Abstract

Knowledge about the demographic and environmental factors underlying population dynamics is fundamental to designing effective conservation measures to recover depleted wildlife populations. However, sparse monitoring data or persistent knowledge gaps about threats make it difficult to identify the drivers of population dynamics. In situations where small, declining, or depleted populations show continued evidence of decline for unknown reasons, integrated population models can make efficient use of available data to improve our understanding of demography, provide fundamental insights into factors that may be limiting recovery, and support conservation decisions. We used mark-resight and aerial survey data from 2004 to 2018 to build a Bayesian integrated population model for the Cook Inlet population of beluga whales (*Delphinapterus leucas*), which is listed as endangered under the U.S. Endangered Species Act. We examined the effects of prey availability and oceanographic conditions on beluga vital rates and conducted a population viability analysis to predict extinction risk across a range of hypothetical changes in beluga survival and reproduction. Our results indicated that while the survival of breeding females (0.97; 95% CI: 0.95–0.99) and young calves (0.92; 0.80–0.98) was relatively high, the survival of nonbreeders (0.94; 0.91–0.97) and fecundity (0.28; 0.22–0.36) may be depressed. Furthermore, our analysis indicates that the population will likely continue to decline, with a 17–32% probability of extinction in 150 years. Our model highlights the utility of integrated population modeling for maximizing the usefulness of available data and identifying factors contributing to the failure of protected populations to recover. This framework can be used to evaluate proposed conservation and recovery efforts for this and other endangered species.

Introduction

Understanding the demographic and environmental factors driving trends in abundance is fundamental to designing effective conservation measures for wildlife populations. However, knowledge about population dynamics is challenging to obtain, particularly for populations that are small, patchily distributed, or difficult to survey. In these situations, individual data streams might indicate that the population is declining without lending insight into the drivers of the

observed trend or might fail to provide sufficient information to detect a trend at all. This can be particularly true for cetacean populations, where challenging survey conditions and cryptic life history stages can lead to insufficient statistical power for detecting trends (Taylor *et al.*, 2007; Boyd & Punt, 2021). Population models that integrate all available data can improve our ability to quantify the importance of various stressors in shaping population dynamics while accounting for uncertainty and variability in underlying ecological processes.

Integrated population models (IPMs; Besbeas *et al.*, 2002; Brooks, King, & Morgan, 2004) constitute a formal framework for combining multiple data sources through a joint likelihood to simultaneously model demographic rates and abundance, often with improved precision and reduced bias (Abadi *et al.*, 2010). IPMs maximize the utility of available data, which are typically expensive to collect on management-relevant time horizons for long-lived species (Regehr *et al.*, 2018; Zipkin & Saunders, 2018), and are useful for conducting population viability analyses (PVA) to quantify the effects of threats and management actions on extinction risk (Beissinger & Westphal, 1998; Converse, Moore, & Armstrong, 2013). The strengths of this approach have inspired several IPM-based PVAs that examine viability across varying climate change or management scenarios for populations of conservation concern (Saunders, Cuthbert, & Zipkin, 2018; Jenouvrier *et al.*, 2020).

While marine mammals tend to be sensitive to environmental variability and anthropogenic disturbance (Moore, 2018), it can be challenging to disentangle the effects of multiple environmental factors that directly or indirectly affect demography. An exemplar of this challenge is the Cook Inlet population of beluga whales (*Delphinapterus leucas*), which declined dramatically during the 1990s (Hobbs *et al.*, 2006) and is listed as endangered under the U.S. Endangered Species Act (ESA). Despite the cessation of hunting since its precipitous decline, aerial survey data suggest that the population continues to decline (Shelden & Wade, 2019). Though a clear cause for the failure of this population to recover has not been identified, the leading hypotheses include reduced prey availability, reduced foraging success due to anthropogenic noise or other disturbance, natural predation, pollution, small population effects, or a combination of factors (Hobbs, Wade, & Shelden, 2015). The lack of empirical demographic estimates and sparse data on threats in previous modeling frameworks (Hobbs, Wade, & Shelden, 2015; Jacobson *et al.*, 2020) have complicated efforts to identify causes of decline and develop targeted conservation actions that advance recovery.

To improve our understanding of factors affecting the demography and viability of Cook Inlet belugas, we built upon the work of Himes Boor *et al.* (2023) to develop a Bayesian IPM-based PVA using mark-resight and aerial survey data from 2004 to 2018. Using all available demographic information within an IPM framework, we estimated the first time-varying annual vital rates for this population, examined the effects of environmental conditions and prey availability on annual vital rates, identified demographic drivers of population dynamics, robustly quantified uncertainty in extinction risk, and assessed extinction risk across a range of hypothetical changes in survival and reproduction. Our model provides insights into the sensitivity of population dynamics to changes in vital rates and environmental conditions, evaluates evidence for putative threats, and establishes a framework to examine the effects of threats and management alternatives on demographic parameters and viability as additional data become available. Our analysis highlights the usefulness of IPMs for capitalizing on available

information and accounting for uncertainty in the factors contributing to wildlife population declines and the failure of this and other protected species to recover.

Materials and methods

Study species

Of the five beluga whale stocks in Alaskan waters, the geographically and genetically isolated population in Cook Inlet, Alaska (Fig. 1), has the lowest abundance. Belugas exhibit life history traits typical of large, long-lived odontocetes (i.e., late maturing with a long inter-birth interval), common to many species of conservation concern. Based on somewhat limited necropsy examinations and mark-recapture observations, females are thought to reach reproductive maturity around age 10 (McGuire *et al.*, 2020; Shelden *et al.*, 2020), with calves remaining dependent until 2–5 years old. Calving begins in late July and extends into October (McGuire *et al.*, 2020). Belugas are known to inhabit coastal and offshore waters of the inlet, and this population likely remains in Cook Inlet year round, aggregating in estuaries and near river mouths to feed on anadromous prey in summer (Shelden *et al.*, 2015). Belugas are adaptive foragers, feeding on a variety of species in Cook Inlet at different times of the year and in various areas of their range, largely influenced by ice cover and freshwater discharge (Moore *et al.*, 2000; Nelson *et al.*, 2018).

Population monitoring data

The population was monitored using land and boat-based mark-resight surveys in Cook Inlet from May through October, 2005–2017, resulting in 1,931 unique sightings of 471 beluga whales identified in the left-side photographic catalog (McGuire *et al.*, 2020). When individuals were observed, it was noted whether they were unambiguously associated with a young of the year (YOY), a calf (age 1–5), or both. Calves and YOY were associated with adult whales in just under 20% of all sightings. In processing the mark-resight observations, calves were assigned age categories based on calf color, size, and the presence of fetal folds (McGuire *et al.*, 2020), with 12 possible classifications based on known age (e.g., YOY, age-1, age-2, etc.) and age with uncertainty (e.g., \leq age-1 or \geq age-2), or “unknown” if calf age could not be determined (see Himes Boor *et al.*, 2023 for more details). Belugas generally only become individually identifiable (using scars or other skin markings) once they are 5 years old or older.

The population was also monitored using aerial surveys annually from 1994 to 2012 and biennially from 2012 to the present, though only data since 2004 were used in this study due to a change in methodology that year (see Boyd *et al.*, 2019). Aerial surveys were conducted strategically, covering 100% of the coastline and approximately half of the inlet over the course of several days, with variable daily survey effort that was spatio-temporally concentrated when and where belugas were thought most likely to be present—

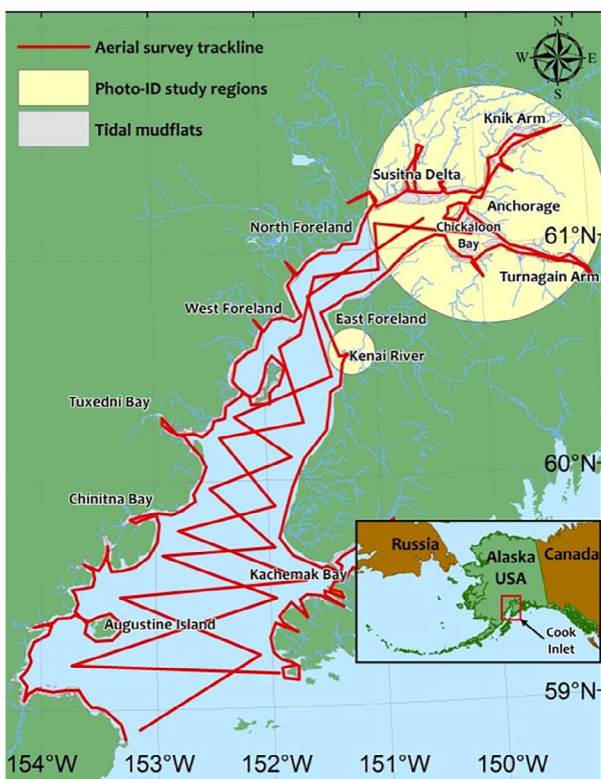


Figure 1 Beluga whale study areas within Cook Inlet, Alaska. Aerial surveys occurred during 2 weeks in June 2004–2018. Photo-identification boat surveys and land-based operations occurred from May–October 2005–2017, primarily north of the Forelands.

near shore at low tide (Shelden & Wade, 2019). Aerial surveys were conducted from twin-engine aircraft with two observers independently recording the number of belugas observed in each encountered group and another observer video recording most counting passes, resulting in daily indices of population size (sum of all surveyed beluga groups, but not corrected for missed groups; Shelden & Wade, 2019, Boyd *et al.*, 2019). The annual population size index was estimated from two to five “acceptable” (defined by weather, sighting conditions, and spatial coverage; Shelden & Wade, 2019) daily aerial survey counts using a Bayesian hierarchical model that accounted for availability, perception, and visibility bias in the daily group counts of encountered groups due to the difficulty of detecting darker, smaller animals in turbid waters and the uncertainty surrounding dive intervals but did not account for missed groups or dispersed individuals (Boyd *et al.*, 2019). The posterior distributions of daily population sizes were summarized to provide a single median estimate and standard deviation for each survey year (see Boyd *et al.*, 2019; Shelden & Wade, 2019), which were used as data in the abundance model described below. Differing assumptions underlying the aerial survey have led to different approaches for estimating the population size index using the median of daily survey counts versus an average of the highest or “maximum” of acceptable daily surveys in

a given year (see Shelden & Wade, 2019). As described in Shelden & Wade (2019), using the median estimate (rather than the highest) as inputs into the integrated model minimizes potential biases that could be introduced by the use of a rank-order statistic. However, use of the median estimate has the potential to underestimate the population size if beluga groups or many dispersed individuals are frequently missed during surveys (Shelden & Wade, 2019); thus, our IPM abundance model described below addresses this potential bias by incorporating a population-level detection parameter.

Statistical analyses

Multi-event model

Himes Boor *et al.* (2023) introduced a multi-event model framework to estimate fecundity and age-specific survival using mark-resight data on individuals with uncertain age. We adapt that original implementation by estimating time-varying demographic rates, applying covariates, and using it within this IPM-based PVA. In brief, the Himes Boor *et al.* (2023) multi-event model includes 14 life history states based on reproductive status (breeder versus nonbreeder) and the number of associated dependent offspring in various age combinations (e.g., “Breeder with YOY & 2YO calves”). Due to the long gestation period and inter-birth interval observed in beluga populations, it is assumed that females cannot give birth in consecutive years (i.e., “Breeder with YOY & 1YO calves” is not a state in the model). The state process is defined as,

$$z_{i,t} | z_{i,t-1} \sim \text{categorical}(\Omega_{z_{i,t-1}, i, t-1})$$

where the state z of individual i at occasion t , conditional on the individual's state at the previous occasion, is categorically distributed according to matrix Ω , which is the product of survival, calf aging, and breeding transition matrices. Stage-specific survival was estimated for four groups: breeding females (females who have given birth to at least one calf; S_B); nonbreeding individuals (age 6^+ belugas, including subadults of both sexes, adult males, and nonbreeding adult females; S_N); younger calves (survival from birth to age 2; S_Y); and older dependent calves (ages 3–5; apparent survival ϕ_C , as true older calf survival is confounded with becoming independent). The survival of young and older calves was conditioned on breeding female survival to account for young calves dying and older calves becoming independent if the female died. Breeding transition matrices allow reproductively mature individuals (age 10^+) to calve for the first time (ψ_N , though this parameter is of limited ecological interest because the pool of individuals referred to collectively as nonbreeders includes males) and thereafter (ψ_B ; e.g., fecundity, which encompasses neonate survival prior to the start of the mark-resight surveys each year).

Each stage-specific demographic rate ξ was modeled as a function of temporally varying covariates and random effects of year,

$$\text{logit}(\xi_a) = \mu_a^\xi + \beta_{a,c}^\xi \cdot x_t^c + \epsilon_{a,t}^\xi$$

where μ_a^ξ is the intercept for demographic rate ξ and age group a , coefficients $\beta_{a,c}^\xi$ describe the effects of covariate c , with value x_t^c at time t , on each vital rate for age group a and $\epsilon_{a,t}^\xi$ are random year effects. All covariates were Z-scored, so the intercept μ_a^ξ represents the vital rate at the mean level of each covariate. Intercepts μ_a^ξ were logit-transformed parameters with uniform(0, 1) prior distributions. To improve parameter estimability and regulate model complexity, we used penalized complexity priors (Simpson *et al.*, 2017) for covariate coefficients and random year effects, which shrink the parameter estimate toward zero in the absence of strong support for larger values. Thus, the random year effects and the effects of covariates were assumed to be drawn from a Gaussian distribution with standard deviations distributed according to an exponential distribution with a fixed shrinkage rate; $\epsilon_{a,t}^\xi \sim \text{normal}(0, \sigma_a^\xi)$ and $\beta_{a,c}^\xi \sim \text{normal}(0, \sigma_{a,c})$ where $\sigma \sim \text{exponential}(\nu = 1)$ in both.

The observation process model accounts for the uncertainty in both female reproductive status and calf age determination. Specifically,

$$y_{i,t} | z_{i,t} \sim \text{categorical}(\Theta_{z_{i,t-1,i,t}})$$

where observations (y) conditional on life history state (z) are categorically distributed with a probability matrix Θ , composed of age-specific detection probabilities and calf age assignment probabilities. Detection probabilities include those for young (δ_Y) and older calves (δ_C) (conditional on detecting the female), nonbreeding subadults and adults (p_N), and breeding females with (p_{B_C}) and without ($p_{B_{Sk}}$) calves. Similar to demographic rates, detection probabilities for each age group a were modeled as

$$\text{logit}(p_a) = \mu_a^p + \beta_p \cdot x_t^p + \epsilon_{a,t}^p$$

$$\text{logit}(\delta_a) = \mu_a^\delta + \beta_\delta \cdot x_t^\delta + \epsilon_{a,t}^\delta$$

where the intercept μ_a^p for each age group a was estimated using a logit-transformed parameter with a uniform (0, 1) prior distribution. Detection rates were modeled separately for each age group because beluga skin color lightens from dark gray to white as they age, and age groups may exhibit stage-specific behavioral differences that affect detectability as well (e.g., females with YOY foraging in different locations, older calves ranging farther from females compared to YOY, etc.). A fixed effect β_p accounted for variable survey effort x_t^p , the Z-scored number of vessel- and land-based surveys that occurred each year. Interannual random effects for each age group were estimated using penalized complexity priors as above, $\epsilon_{a,t}^p \sim \text{normal}(0, \sigma_p)$ and $\sigma_p \sim \text{exponential}(\nu = 1)$.

The parameters describing calf age assignment probability given the calf's true age, discussed in detail by Himes Boor *et al.* (2023), included the probabilities of assigning an individual to an age category (as opposed to "unknown"; γ), assigning calf age with perfect certainty (e.g., age 1 when YOY was observed with certainty; α), assigning an uncertain

age that matches the true age (e.g., YOY assigned to \geq age-1 category; ω), assigning an uncertain age different than the true age by 1 year (e.g., age-1 individual assigned \leq age-2 category; κ), and the probability of true age being at the upper limit of the assigned age category (e.g., yearling calf placed in the ≤ 1 year old category; η).

Abundance model

The second component of this IPM is the state-space model for estimating annual population size using aerial survey data. To account for the high variability in annual aerial survey counts due to the difficulty of detecting some belugas and grouping behavior depending on tidal flux, population size is modeled as,

$$\widehat{N}_{\mu_t} \sim \text{normal}(N_t, \widehat{\sigma}_t)$$

$$N_t \sim \text{binomial}(N_{\text{Tot}}, p_{\text{Ab}_t})$$

where the annual median aerial survey population size index, \widehat{N}_{μ_t} , is modeled as arising from a normal distribution with a mean equal to N_t (the population size in year t subject to detection in the aerial survey) and with a standard deviation $\widehat{\sigma}_t$. In turn, N_t is modeled as arising from a binomial distribution with index equal to the total abundance, N_{Tot} , from the IPM process model, and the aerial survey detection probability, p_{Ab_t} , estimated with prior Beta (1, 1). This structure takes into account the potential for the abundance indices used as data (i.e., \widehat{N}_{μ_t}) to be negatively biased as a result of unsurveyed portions of the population. The annual estimates \widehat{N}_{μ_t} and their sampling standard deviations $\widehat{\sigma}_t$ estimated previously (Boyd *et al.*, 2019; Shelden & Wade, 2019) were used here as data instead of fully integrating the raw daily aerial survey counts due to the computational burden and complexity of estimating availability, perception, and proximity biases that underlie the annual abundance indexes. Due to the uncertainty surrounding the degree to which underlying assumptions in the aerial survey are met (namely the lack of data informing the proportion of the population missed on a given survey day and whether groups are systematically versus randomly missed), we examined the sensitivity of demographic parameter estimates to the prior used for the aerial survey detection probability, p_{Ab_t} , and to the use of "maximum" versus "median" daily aerial survey counts (Appendix S1; see Shelden & Wade (2019) for additional details). As there is often additional auxiliary data informing the estimation of detection probability within a binomial observation process model within an IPM, we examined the identifiability of this structure with the proportional overlap between the prior and posterior distributions of p_{Ab_t} (Gimenez, Morgan, & Brooks, 2009).

Integrated model

Abundance for each age group and life history state were modeled using stochastic population growth equations with

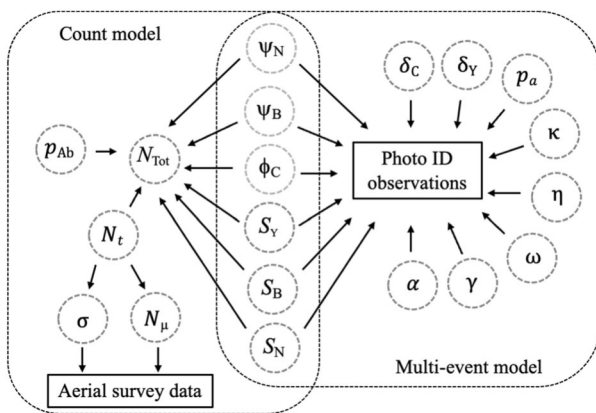


Figure 2 Directed acyclic graph of the integrated population model framework for Cook Inlet beluga whale abundance (N_{Tot}), including (a) the multi-event mark-recapture model estimating fecundity (ψ_N , ψ_B) and the survival of breeding females (S_B), nonbreeding subadults/adults (S_N), and calves (S_Y , ϕ_C), and stage a specific detection probabilities for independent groups (p_a) and dependent calves (δ_C , δ_Y), and age classification error parameters (α , γ , ω , η , κ) (b) the count model estimating group size (N_t) based on aerial survey counts (N_μ) and standard deviation (σ) and the associated detection probability (p_{Ab}).

vital rate and population size estimates from the two sub-component models (Fig. 2). The age at which females could enter the breeding population (i.e., age at potential first birth; DeMaster, 1981) was set at 10 years, though we examined the sensitivity of model results to a range of potential ages at first birth (Appendix S2). The age structure in the first model year was established using a multinomial distribution based on the assumption of a stable age distribution. In each subsequent year t , the number of individuals in the YOY age group was equal to the number of females with YOYs in that year, and the numbers of individuals in all other age groups and breeding states were modeled as binomial outcomes given survival and breeding transition probabilities and abundances in the previous year:

The number of older calves is the sum of individuals aged 3–5: $N_{C_t} = \sum(N_{3,5,t})$. The number of juveniles is the sum of individuals aged 6–9: $N_{J_t} = \sum(N_{6,9,t})$. The number of established breeders age 10⁺ with a YOY in year $t + 1$ ($N_{B_{YOY,t+1}}$) is composed of first-time breeders ($\text{Bin}(N_9, S_{N_t} \cdot \psi_N)$), previous nonbreeders age 10⁺ transitioning to the calving group ($\text{Bin}(N_{NB_t}, S_{N_t} \cdot \psi_N)$), and previously established breeders without a YOY in year t (i.e., “skipping”) calving again ($\text{Bin}(N_{B_{Sk_t}}, S_{B_t} \cdot \psi_B)$). The number of established breeders without a YOY in year $t + 1$ ($N_{B_{Sk,t+1}}$) is composed of surviving breeders with a YOY in year t ($\text{Bin}(N_{B_{YOY_t}}, S_{B_t})$) and previous “skipping” breeders not calving ($\text{Bin}(N_{B_{Sk_t}}, S_{B_t} \cdot (1 - \psi_B))$). The number of nonbreeders ($N_{NB,t+1}$) is composed of age-10 individuals that did not calve ($\text{Bin}(N_9, S_{N_t} \cdot (1 - \psi_N))$) and surviving previous age 10⁺ nonbreeders that again did not calve ($\text{Bin}(N_{NB_t}, S_{N_t} \cdot (1 - \psi_N))$). Total abundance in each year was calculated as the sum of all (st)ages: YOY (N_{YOY_t}), younger calves age 1–2 ($N_{1,2,t}$), older calves age 3–5 ($N_{3,4,5,t}$), juveniles age 6–9 ($N_{6,7,8,9,t}$), nonbreeders age 10⁺ (N_{NB_t}), and established breeders with YOY ($N_{B_{YOY_t}}$) and without YOY ($N_{B_{Sk_t}}$): $N_{Tot} = \sum(N_{stage_t})$.

Environmental covariates

To examine the effects of environmental variability and prey availability on beluga demography, we selected two covariates: sea surface temperature (SST) and a metric of prey biomass. We selected SST as a covariate because it is one of the strongest features of atmospheric processes that have been identified as predictors for the growth of various salmon and groundfish species (i.e., NPGO, PDO; Litzow *et al.*, 2018) that are important beluga prey (Quakenbush *et al.*, 2015). It should be noted, however, that SST in the Gulf of Alaska may not reflect conditions experienced by belugas in upper Cook Inlet, where conditions are strongly influenced by river features and tidal fluctuations. Monthly Gulf of Alaska SSTs were compiled from a large geographic space (approximately 54 to 60°N and 137 to 157°W) using the NOAA GOES satellite data accessed from ERDDAP (Simons, 2019) and averaged to produce annual

$$\begin{aligned}
 N_{YOY_{t+1}} &= N_{B_{YOY,t+1}} \\
 N_{1_{t+1}} &\sim \text{Bin}(N_{YOY_t}, S_{Y_t}) \\
 N_{2_{t+1}} &\sim \text{Bin}(N_{1_t}, S_{Y_t}) \\
 N_{3_{t+1}} &\sim \text{Bin}(N_{2_t}, \phi_{C_t}) \\
 N_{4_{t+1}} &\sim \text{Bin}(N_{3_t}, \phi_{C_t}) \\
 N_{5_{t+1}} &\sim \text{Bin}(N_{4_t}, \phi_{C_t}) \\
 N_{6_{t+1}} &\sim \text{Bin}(N_{5_t}, \phi_{C_t}) \\
 N_{7_{t+1}} &\sim \text{Bin}(N_{6_t}, S_{N_t}) \\
 N_{8_{t+1}} &\sim \text{Bin}(N_{7_t}, S_{N_t}) \\
 N_{9_{t+1}} &\sim \text{Bin}(N_{8_t}, S_{N_t}) \\
 N_{B_{YOY,t+1}} &= \text{Bin}(N_9, S_{N_t} \cdot \psi_N) + \text{Bin}(N_{NB_t}, S_{N_t} \cdot \psi_N) + \text{Bin}(N_{B_{Sk_t}}, S_{B_t} \cdot \psi_B) \\
 N_{B_{Sk,t+1}} &= \text{Bin}(N_{B_{YOY_t}}, S_{B_t}) + \text{Bin}(N_{B_{Sk_t}}, S_{B_t} \cdot (1 - \psi_B)) \\
 N_{NB,t+1} &= \text{Bin}(N_9, S_{N_t} \cdot (1 - \psi_N)) + \text{Bin}(N_{NB_t}, S_{N_t} \cdot (1 - \psi_N))
 \end{aligned}$$

means spanning October of year t to September of year $t + 1$ to align with the survey season and beluga reproductive cycle.

The multispecies prey biomass metric was derived by compiling summer in-river reconstructed run estimates for Chinook (*Oncorhynchus tshawytscha*), escapement counts for coho (*O. kisutch*), chum (*O. keta*), sockeye (*O. nerka*), and pink salmon (*O. gorbuscha*), and recreational harvest of eulachon (*Thaleichthys pacificus*) from areas within the Susitna Delta, Knik Arm, and Chinitna Bay in Cook Inlet (Alaska Department of Fish & Game, 2021). Fish counts were multiplied by species-specific average weights and energy content (O'Neill, Ylitalo, & West, 2014), summed across all species, and then Z-scored and scaled for an overall index of prey biomass. Both covariates were applied to fecundity and survival rates in year t . In addition to reporting the median logit-scale effect size, we also report the probability of the coefficient being above or below zero for each covariate coefficient $\beta_{a,c}^{\xi}$, based on its posterior distribution.

We compared the fit of a “full” model that included both covariates to a base model without covariates using the Watanabe-Akaike information criterion (WAIC; Watanabe, 2010). We conducted the PVA (see below) using the base model to align with our intention of examining covariates in an exploratory manner only, due to the uncertain link between covariates and demography and the challenges of projecting covariates forward in time. In addition to these two primary covariates, an expanded analysis of other covariates, including additional oceanographic indices, species-specific prey biomass, and proxies for other stressors, is provided in Appendix S3.

Model fitting

The model was fitted in JAGS (Plummer, 2019) using package jagsUI (Kellner, 2019) in the R programming language (R Core Development Team, 2022), with code to reproduce the analyses available on GitHub (Warlick *et al.*, 2023). Posterior distributions were calculated using Markov Chain Monte Carlo (MCMC) estimation with three chains run for 40 000 iterations after a burn-in of 30 000 iterations with a thinning rate of 2, resulting in 15 000 MCMC samples. We evaluated model convergence with visual inspection and the Brooks-Gelman-Rubin statistic (Gelman & Rubin, 1992) $\hat{R} < 1.1$. As goodness of fit tests are not well developed for multi-event models (Pradel, Gimenez, & Lebreton, 2005), and due to the complexity of the multi-event model implemented here (large number of possible observation events), we did not evaluate goodness of fit on that subcomponent model. Instead, we evaluated model fit using a posterior predictive check (Kéry & Schaub, 2012) for total abundance (simulated new N_t^{pp} based on the posterior distribution of N_t and then drew new $\hat{N}_{\mu_t}^{pp}$ from a normal distribution with mean N_t^{pp} and standard deviation $\hat{\sigma}_t$), which indicated a reasonable fit (Fig. 3a).

Population growth rates, sensitivity, and viability analyses

Using results from the model fit without covariates, we examined the sensitivity of population growth to

demography by estimating the correlation coefficient (r) between the annual population growth rate, $\lambda_t = \frac{N_{Tot,t+1}}{N_{Tot,t}}$, and annual fecundity and survival probabilities. For each demographic rate, we calculated r for each MCMC chain sample and the proportion that was above versus below zero (i.e., the probability that the correlation coefficient was positive or negative).

To examine future viability, we projected the population forward for 150 years (a time horizon we chose given the delay between the onset of unsustainable demographic rates and extinction in long-lived species) using the posterior distributions for demographic rates and age-specific abundances. To delineate between environmental stochasticity and parametric uncertainty in population projections (White, 2000; Ellner & Fieberg, 2003), 500 projections were conducted for each of the 15 000 MCMC samples from the posterior distribution of the IPM, for a total of 7 500 000 population trajectories. For each sample from the posterior distribution, the estimated deviates from the random effect distributions, $\epsilon_{a,t}^{\xi}$, for the 12 years informed by mark-resight data were jointly (to maintain covariance) randomly sampled with replacement and used to simulate all survival and breeding probabilities in each year of the projection, representing a demographic “status quo.” This approach was used because generating demographic rates from a logit-normal distribution with an estimated mean very close to 1.0 on the probability scale (i.e., for female breeding survival) sometimes resulted in unreasonably low random deviates, well below any observed annual survival rates. By using observed deviates, we restricted survival probabilities to biologically plausible values, and for consistency, we followed this approach for the other demographic parameters. To examine the effect of potential changes in demographic rates on viability, we also projected the population forward as described above under all possible combinations of three hypothetical percent increases in vital rates (e.g., a 1% increase raises survival from 0.90 to 0.909): 1, 1.5, or 2% for adult survival; 1, 2, or 4% for young calf survival; and 5, 10, or 15% for older calf survival and fecundity. These percent increases were chosen based on the estimated temporal variability in each vital rate and also to reflect ecological theory (e.g., fecundity and independent calf survival will be more variable than the survival of adults and dependent calves). Summary statistics (arithmetic mean and upper and lower quantiles) for annual growth rates were calculated across the 7 500 000 population projections, and geometric mean population growth rates were calculated across years.

We summarized the posterior distributions of population projections in terms of the probability of extinction, $\text{Pr}(N_{Tot} < 2)$; the probability of having no remaining breeding females, $\text{Pr}(N_B < 1)$; the probability of exceeding the ESA downlisting criterion of 520 individuals, $\text{Pr}(N_{Tot} > 520)$; the average population growth rate, λ ; and the probability of population growth, $\text{Pr}(N_{Tot,2004} < N_{Tot,2168})$. Additionally, we estimated a quasi-extinction threshold (Appendix S4) as called for in the Cook Inlet beluga whale Recovery Plan (NMFS, 2016).

Results

Demographic rates

The posterior median of the intercept parameter (grand mean over study period years) for breeding female survival (μS_B) was 0.97 (95% credible interval: 0.95–0.99; Table 1) based on inference from the model that included temporal variance but did not include environmental covariates. The posterior median of the intercept parameter for non-breeding adult survival (μS_N), which includes older juveniles, non-breeding adult females, and adult males was 0.94 (0.91–0.97). The posterior median of young calf survival (μS_Y) across the study period was approximately 0.92 (0.80–0.98). The posterior median of apparent survival of older calves ($\mu \phi_C$) was approximately 0.56 (0.35–0.79). The posterior median of fecundity ($\mu \psi_B$; breeding probability for previously established breeders), was 0.28 (95% CI: 0.22–0.36) over the study period (Table 1), ranging from a low of 0.22 in 2011–2012 to a high of 0.35 in 2013. Demographic rate estimates varied little across the range of possible ages of first reproduction (Appendix S2). Detection and state assignment probabilities from the mark-resight model were variable and dependent on state (Appendix S5).

Abundance

During the period informed by data (2004–2021), the average population growth rate λ was 1.00 yr^{-1} (95% credible interval: 0.91–1.09), though the population increased at a rate of 1.01 yr^{-1} (0.92–1.09) from 2004–2010 and subsequently declined at a rate of 0.99 yr^{-1} (0.89–1.07) from 2011–2021. Annual mean abundance estimates were generally >400

individuals during the early part of the study period and started declining in 2010 to reach 371 (29–455) individuals in 2018 (Fig. 3a). Abundance estimates were somewhat sensitive to the choice of prior for detection probabilities in the population size model, with the most informative prior distribution leading to a lower posterior median abundance estimate in the final year compared with the estimates using the flat or weakly informative priors (Appendix S1).

Sensitivity and viability analyses

Demographic rates showed moderate to weak correlations with annual population growth, λ_t , with fecundity ($r = 0.49$; 95% credible interval: −0.14 to 0.83) and breeding adult survival ($r = 0.47$; −0.2 to 0.83; Fig. 4) being the strongest. Younger and older calf survival were more weakly correlated with population growth, with $r = 0.45$ (−0.21 to 0.83) and $r = 0.44$ (−0.22 to 0.83), respectively. Estimates of nonbreeder survival were not correlated with population growth ($r = 0.26$; −0.38, 0.72).

Over 7 500 000 150-year population projections, the population had a 99% probability of decline (Fig. 3b), with a geometric mean population growth rate of approximately 0.984 (0.982–0.986). The mean probability of extinction, $\Pr(N_{\text{Tot}} < 2)$, was 4% (2–6%) 100 years into the future and 24% (17–32%) 150 years into the future (Table 1). The probability of having no breeding females remaining in the population, $\Pr(N_B < 1)$, was 30% (23–39%) 150 years into the future. The probability of exceeding the ESA downlisting criterion at any point during the study period was 2% (0.8–5%).

In examining how changes in demography affected population viability, abundance trajectories were most strongly affected by changes in the survival of breeding females and

Table 1 Posterior median and 95% credible interval (CI) estimates for demographic parameters and viability metrics for Cook Inlet beluga whales in Alaska, developed using an integrated population model based on data from 2004 to 2018

Parameter	Description	Median	CI
μS_B	Female breeder survival	0.97	0.95–0.99
μS_N	Nonbreeding survival	0.94	0.91–0.97
$\mu \phi_C$	Apparent older calf survival	0.56	0.35–0.79
μS_Y	Young calf survival	0.92	0.80–0.98
$\mu \psi_B$	Fecundity	0.28	0.22–0.36
$\mu \psi_N$	First-time breeding probability	0.07	0.06–0.09
μp_N	Nonbreeder detection	0.47	0.38–0.56
μp_{Bc}	Breeder with calf detection	0.67	0.53–0.79
μp_{BN}	Breeder without calf detection	0.74	0.60–0.88
$\mu \delta_C$	Older calf detection	0.44	0.33–0.56
$\mu \delta_Y$	Young calf detection	0.55	0.45–0.64
p_{Ab}	Aerial survey detection probability	0.76	0.62–0.90
$N_{\text{Tot}2018}$	Abundance in 2018	371	295–455
λ	Population growth rate (geometric mean)	0.98	0.982–0.986
$\Pr(N_{\text{Tot}2168} < N_{\text{Tot}2004})$	Probability of decline (150 years)	0.99	0.98–0.99
$\Pr(N_{\text{Tot}} < 2)_{2118}$	Extinction probability (100 years)	0.04	0.02–0.06
$\Pr(N_{\text{Tot}} < 2)_{2168}$	Extinction probability (150 years)	0.24	0.17–0.32
$\Pr(N_B < 1)_{2168}$	Probability of no remaining breeding females (150 years)	0.30	0.23–0.39
$\Pr(N_{\text{Tot}} > 520)_{2018:2168}$	Probability of exceeding downlisting criterion	0.02	0.008–0.05

Parameters preceded by the μ symbol are those modeled with temporal variance, with the estimated mean intercept reported here.

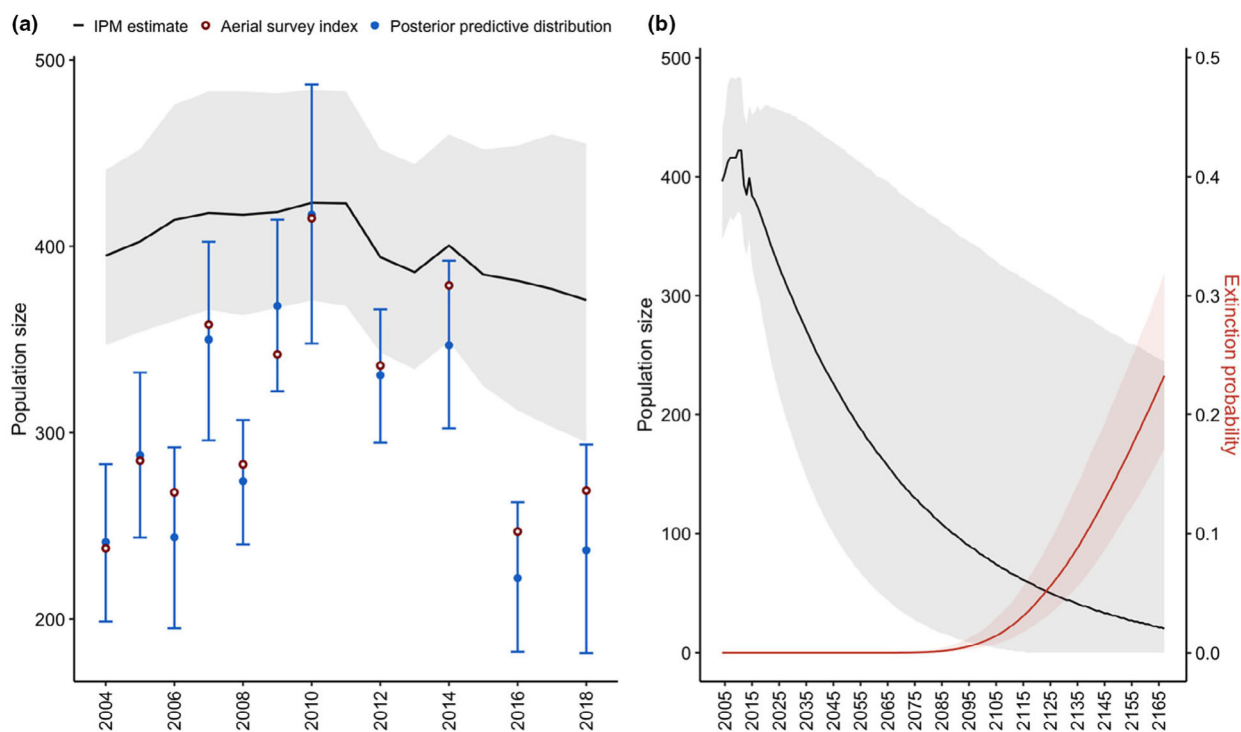


Figure 3 (a) Predicted population abundance (N_{Tot} ; black line), 95% credible interval (gray shading), population size index based on aerial survey data during the study period (N_{μ} ; red circles), and posterior predictions for population size subjected to aerial survey detection (N_{δ} ; blue dots and error bars), and (b) projected abundance and annual extinction probability over a 150-year period for Cook Inlet belugas based on estimated demographic rates and abundance from mark-resight (2005–2017) and aerial survey (2004–2018) data.

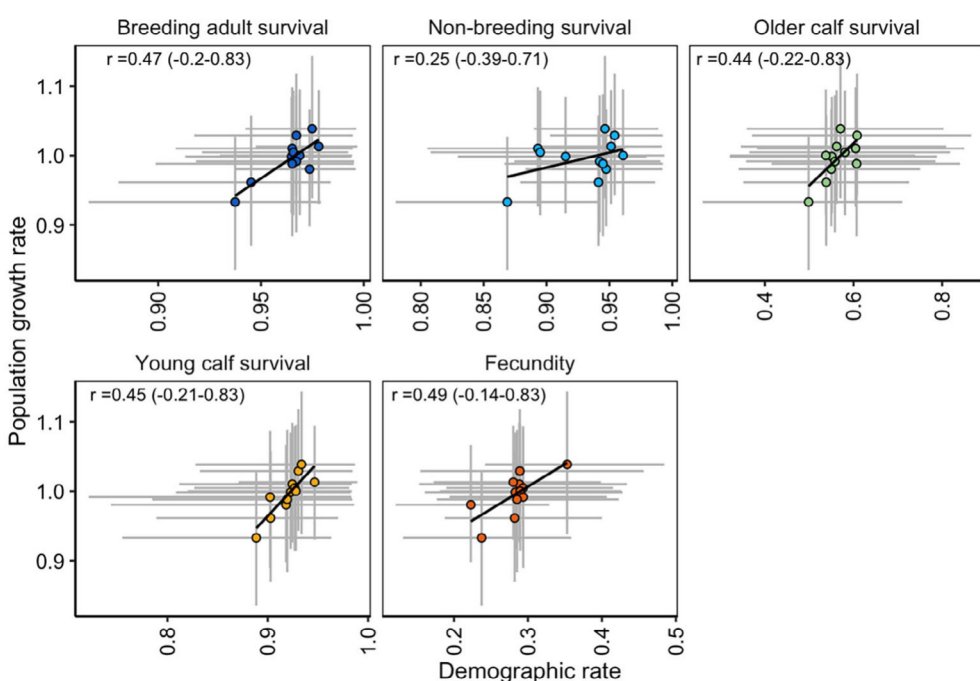


Figure 4 Posterior median (colored dots) and 95% credible intervals (gray bars) for annual population growth rates and demographic rates during the study period (2004–2018) as estimated by the Bayesian integrated population model, with posterior median correlation coefficients, r , and 95% credible intervals shown in parentheses for fecundity and adult, older calf, and young calf survival for beluga whales in Cook Inlet, Alaska.

nonbreeding subadults/adults (Fig. 5a). Geometric mean population growth rates exceeded 1.0 when breeding female and nonbreeding subadult and adult survival were increased by at least 1.5% in addition to some other combination of demographic rate increases (Fig. 5b). The probability of extinction at 150 years was reduced from the baseline of 24 to 1.9% with a 2% increase in adult survival and to 1.5% with a simultaneous 2% increase in young calf survival and a 15% increase in fecundity. To give context to these percent changes, a 2% increase in adult survival would correspond to an average of an additional three breeding females surviving any given year, based on the population size and structure in 2018 at the end of the data period (i.e., $\mu S_B \times 1.02 \times N_{B2018} \approx 3$). Similarly, a 10% increase in fecundity would correspond to one additional birth.

Environmental covariate effects

Fecundity was positively correlated with Gulf of Alaska SST ($\beta_{SST} = 0.23$; 95% CI = −0.06 to 0.65; $Pr(\beta_{SST} > 0) = 0.92$) and the index of prey biomass ($\beta_{prey} = 0.14$; −0.04 to 0.40; $Pr(\beta_{prey} > 0) = 0.91$). Notable correlations were not apparent between either covariate and adult or calf survival probabilities. Though effect sizes were relatively small, the inclusion of Gulf of Alaska SST and the index of prey biomass resulted in improved model fit compared to when covariates were excluded ($\Delta_{WAIC} = -5$ relative to the model

with temporal variance only; $\Delta_{WAIC} = -180$ relative to the null model without temporal variance or covariates).

Discussion

We developed a Bayesian IPM-based PVA to evaluate drivers of population dynamics and the future viability of Cook Inlet belugas, a population that has failed to recover from past depletion despite its protected status. Based on our results, the population has declined since 2011 to an abundance of 371 (295–455) individuals as of 2018. The population is projected to decline at an average rate of 1.6% per year in the coming decades, assuming constant environmental variability and that vital rates remain the same as during the latter part of the study period rather than being more similar to pre-2011 conditions. This projected trend results in a 2–6% probability of extinction over the next 100 years, a 17–32% probability of extinction over the next 150 years, and a 2% probability that the population will meet the criterion for downlisting from endangered to threatened.

The extinction risk reported here is likely an underestimate, as our model does not account for changing climate, potential mortality due to catastrophic events, or factors such as inbreeding depression or allele effects that can hamper the recovery of very small populations (Lande, 1988). Ultimately, the population is unlikely to experience positive growth unless conservation actions can be identified that will

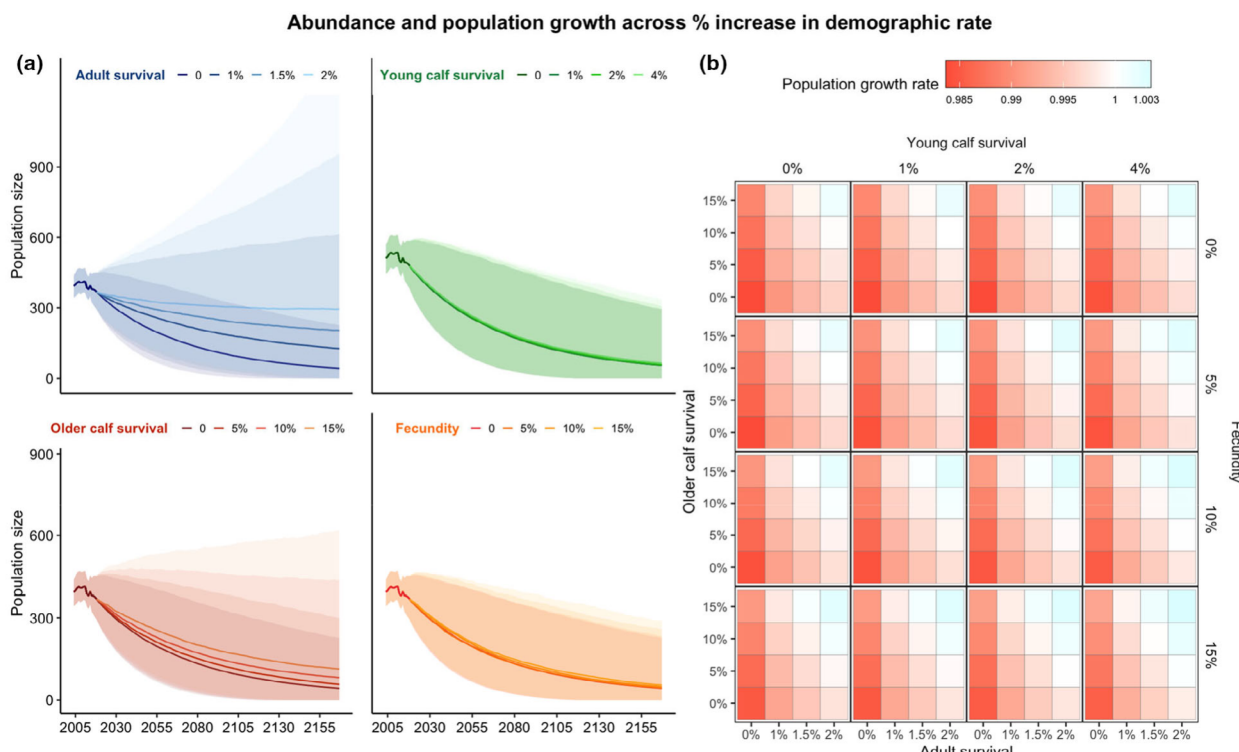


Figure 5 (a) Estimated (2004–2018) and projected (2019–2067) abundance for Cook Inlet beluga whales in Alaska using a Bayesian integrated population model across a range of demographic changes when all other demographic rates are held constant, and (b) negative versus positive population growth rates (red-blue color scale) over hypothetical percent increases in demographic rates.

promote and maintain higher rates of adult survival and fecundity. Though a paucity of data about stressors remains a barrier, our IPM provides a framework for testing hypotheses about threats and evaluating management alternatives in the future when additional data becomes available. From a methodological perspective, annual abundance estimates from our IPM highlight the value of contributing additional information (i.e., the mark-resight data) beyond the aerial survey data to the estimation of abundance, particularly at the start and end of the study period (Fig. 3a). This emphasizes the importance of continuing to collect long-term mark-resight or other demographic data and using IPMs to incorporate all available data to maximize the precision of abundance estimates for this and other marine mammal populations.

Understanding a population's sensitivity to changes in demographic rates is fundamental to developing hypotheses about factors that underlie changes in abundance. For long-lived mammals with delayed maturity and high maternal investment, ecological theory and empirical evidence suggest that adult survival is a stronger driver of population dynamics than juvenile survival or fecundity (Heppell, Caswell, & Crowder, 2000; Runge, Langtimm, & Kendall, 2004). Our results indicated that young calf survival (estimated with temporal variance for the first time here) and breeding adult survival were high and similar to rates reported for other stable cetacean populations (Jordaan *et al.*, 2020). It is therefore unlikely that increasing breeding female survival is a logistically practical or biologically feasible way to bolster population growth. Nonbreeder survival was lower than that of breeding females (not entirely unexpected given the group included subadults) and consistent with estimates for subadults and adults in the declining beluga population in the St. Lawrence Estuary, Canada (Mosnier *et al.*, 2015) and other depleted, declining, or hunted cetacean populations (Luque & Ferguson, 2010). Additionally, estimated fecundity (0.28, 0.22–0.36; equivalent to a 4.6-year inter-birth interval) was lower than that previously estimated for this and other beluga populations (2- to 3-year inter-birth interval; Jacobson *et al.*, 2020; Mosnier *et al.*, 2015). Despite the theoretical importance of adult survival for long-lived species, fecundity rates generally exhibit greater fluctuations (Gaillard, Festabianchet, & Yoccoz, 1998) and are more sensitive to environmental variability (Benton & Grant, 1996), and therefore likely have greater potential to increase, as was found for Southern Resident killer whales (*Orcinus orca*; Lacy *et al.*, 2017) and bottlenose dolphins (*Tursiops aduncus*; Manlik *et al.*, 2016). Our results suggest that increasing fecundity and calf survival alone would be unlikely to reverse the declining trend, but that increasing these while also maintaining high rates of breeding female and nonbreeding subadult and adult survival would improve the viability of Cook Inlet belugas. However, identifying and implementing conservation actions that might facilitate achieving those targets is challenging, particularly given the greater degree of uncertainty in the survival of older calves, which is partially a function of the fact that apparent survival in this age group cannot be fully distinguished from the probability that an older calf becomes independent.

Even when conservation actions can be designed to ameliorate the impact of threats, the efficacy of these measures is often hindered by underlying environmental variability. Our results indicated that the fecundity and survival rates of Cook Inlet belugas are likely affected by prey abundance and oceanographic conditions. Over the study period, survival and fecundity were lower during 2011 and 2012 (Figure S5.1), suggesting that environmental conditions may have been suboptimal or anthropogenic stressors more acute in those years. The productivity of Chinook salmon populations throughout Cook Inlet from 2003 to 2007 was poor due to adverse freshwater conditions, which contributed to diminished returns of adult salmon in subsequent years (Jones *et al.*, 2020). Despite the uncertainty in the spatio-temporal alignment of available prey data and beluga foraging, it is conceivable that these trends impacted foraging conditions, particularly during late gestation and lactation when energetic demands are high.

In terms of SST, Arimitsu *et al.* (2021) concluded that the 2014–2016 marine heatwave in the northern Gulf of Alaska led to declines in forage species, leading to large-scale declines in abundance and breeding success of salmon, groundfish, birds, and mammals. It is therefore challenging to identify the mechanism(s) by which warmer ocean conditions would generally correlate with slightly higher beluga survival and reproduction, as indicated by our analysis. However, as an underlying component of basin-scale atmospheric processes that affect both physical (e.g., winds, currents, and storms) and biological (e.g., nutrient concentrations, prey abundance) processes, it is possible that elevated SST confers benefits (up to a point) as a shorter-term foraging cue or coincides with the availability of preferred prey. However, these somewhat ambiguous findings related to the effects of SST exemplify the challenges of understanding the ecological scale at which oceanographic conditions are most meaningful for top predators. For this small and isolated population of whales that forage primarily in the upper Cook Inlet, it may be that prey availability and environmental conditions are more strongly influenced by highly localized processes such as river outflow compared with broadscale climatic patterns.

For long-lived top predators that are able to switch target prey or move to avoid disturbances, it is difficult to identify a single root cause of decline and challenging to quantify the synergistic effects of multiple stressors. For Cook Inlet belugas, it could be that underwater noise reduces foraging opportunities in situations where prey availability is already diminished, hindering the recovery of the population after decades of hunting pressure. It could also be that pollution reduces resilience against illness and disease. Unfortunately, the paucity of spatially explicit data on threats, beluga health, and demography generally precludes a robust examination of these hypotheses. Though we examined the effects of additional anthropogenic stressors and the season-specific effects of environmental conditions, a more nuanced understanding of cumulative effects and the strength, duration, and lag times of environmental effects could be explored in future research.

The rapid decline of this population and the difficulty in obtaining data on anthropogenic threats together highlight

the importance of developing recovery strategies despite the all-too-common limitations of missing or imperfect information. In an examination of the threats facing over 150 species listed under the ESA, more than one-third of the associated recovery plans lacked information about either the magnitude, timing, frequency, or severity of the threats (Lawler *et al.*, 2002). Identifying conservation measures that aim to mitigate a combination of stressors is challenging but essential: if the cumulative effects of multiple threats are driving declines, as outlined in the Recovery Plan for Cook Inlet belugas (NMFS, 2016), interventions targeting only a single threat would likely need to reduce the impacts of that threat to implausibly low levels to counteract other stressors (Rhodes *et al.*, 2011; Pirotta *et al.*, 2022). In a recent viability analysis for St. Lawrence Estuary belugas, which are also assumed to suffer from the cumulative effects of multiple stressors (Lesage, 2021), Williams *et al.* (2017) found that the projected decline was only reversed in simulation scenarios where the three greatest stressors (noise, pollution, and reduced prey) were simultaneously addressed.

The IPM-based PVA framework presented here can be used in the future to evaluate and understand the implications of threats to this population. This work provides novel insights into temporal variance in demography, the effects of environmental variability, and the sensitivity of Cook Inlet beluga population dynamics and viability to changes in vital rates. This foundational information and our modeling approach also provide a framework for evaluation of proposed conservation and recovery efforts. Our approach highlights the importance and means of capitalizing on the significant resources that have already been dedicated to monitoring declining populations so that tangible measures can be implemented to understand and reverse the current trajectory of this and other endangered populations.

Acknowledgments

This work would not have been possible without the tremendous effort and dedication of research teams from the Cook Inlet PhotoID Project and from NOAA Fisheries. Aerial surveys were conducted under NMFS Scientific Research Permits 782–1719, 14245, and 20465. CIBW photo-ID surveys were conducted under General Authorization, Letter of Confirmation No. 481-1759, and NMFS Scientific Research Permits 14210 and 18016. The authors would like to thank the National Science Foundation Graduate Research Fellowship and the Cooperative Institute for Climate, Ocean, and Ecosystem Studies (CICOES) at the University of Washington for facilitating funding for A.J. Warlick through NOAA Stock Assessment Analytical Methods. G.K. Himes Boor was funded in part by Tribal Wildlife grant no. F22AP00681-00 to the Knik Tribe from the U.S. Fish and Wildlife Service. The findings and conclusions of the NOAA authors in the paper are their own and do not necessarily represent the views of the National Marine Fisheries Service or NOAA. Any use of trade, firm, or product names is for descriptive purposes only and does not imply endorsement by the U.S. Government. We thank R. Taylor and two

anonymous reviewers for their comments, which greatly improved this manuscript.

Author contributions

A. J. Warlick, A. E. Punt, and S. J. Converse conceived the ideas and designed methodology; G. K. Himes Boor, T. L. McGuire, K. E.W. Shelden, and P. R. Wade collected and curated data contributions; E. K. Jacobson, C. Boyd, and K. E.W. Shelden reviewed methodology; and A. J. Warlick conducted the formal analysis and led manuscript development. All authors contributed critically to the drafts and gave final approval for publication.

References

- Abadi, F., Gimenez, O., Arlettaz, R. & Schaub, M. (2010). An assessment of integrated population models: bias, accuracy, and violation of the assumption of independence. *Ecology* **91**, 7–14.
- Alaska Department of Fish & Game. (2021). Fish count data search. <https://www.adfg.alaska.gov/sf/FishCounts/>
- Arimitsu, M.L., Piatt, J.F., Hatch, S., Suryan, R.M., Batten, S., Bishop, M.A., Campbell, R.W., Coletti, H., Cushing, D., Gorman, K., Hopcroft, R.R., Kuletz, K.J., Marsteller, C., McKinstry, C., McGowan, D., Moran, J., Pegau, S., Schaefer, A., Schoen, S., Straley, J. & von Biela, V.R. (2021). Heatwave-induced synchrony within forage fish portfolio disrupts energy flow to top pelagic predators. *Glob. Chang. Biol.* **27**, 1859–1878.
- Beissinger, S.R. & Westphal, M.I. (1998). On the use of demographic models of population viability in endangered species management. *J. Wildl. Manage.* **62**, 821.
- Benton, T.G. & Grant, A. (1996). How to keep fit in the real world: elasticity analysis and selection pressures on life histories in variable environments. *Am. Nat.* **147**, 115–139.
- Besbeas, P., Freeman, S.N., Morgan, B. & Catchpole, E.A. (2002). Integrating mark-recapture-recovery and census data to estimate animal abundance and demographic parameters. *Biometrics* **58**, 540–547.
- Boyd, C., Hobbs, R.C., Punt, A.E., Shelden, K.E.W., Sims, C.L. & Wade, P.R. (2019). Bayesian estimation of group sizes for a coastal cetacean using aerial survey data. *Mar. Mamm. Sci.* **35**, 1322–1346.
- Boyd, C. & Punt, A.E. (2021). Shifting trends: detecting changes in cetacean population dynamics in shifting habitat. *PLoS One* **16**, e0251522.
- Brooks, S.P., King, R. & Morgan, B.J.T. (2004). A Bayesian approach to combining animal abundance and demographic data. *Anim. Biodivers. Conserv.* **27**, 515–529.
- Converse, S.J., Moore, C.T. & Armstrong, D.P. (2013). Demographics of reintroduced populations: estimation, modeling, and decision analysis. *J. Wildl. Manage.* **77**, 1081–1093.
- DeMaster, D.P. (1981). Estimating the average age of first birth in marine mammals. *Can. J. Fish. Aquat. Sci.* **38**, 237–239.

- Ellner, S.P. & Fieberg, J. (2003). Using PVA for management despite uncertainty: effects of habitat, hatcheries, and harvest on salmon. *Ecology* **84**, 1359–1369.
- Gaillard, J.M., Festa-Bianchet, M. & Yoccoz, N.G. (1998). Population dynamics of large herbivores: variable recruitment with constant adult survival. *Trends Ecol. Evol.* **13**, 58–63.
- Gelman, A. & Rubin, D.B. (1992). Inference from iterative simulation using multiple sequences. *Stat. Sci.* **7**, 457–472.
- Gimenez, O., Morgan, B.J.T. & Brooks, S.P. (2009). Weak identifiability in models for mark-recapture-recovery data. In *Modeling demographic processes in marked populations*. Environmental and Ecological Statistics. Thomson, D.L., Cooch, E.G. & Conroy, M.J. (Eds). Vol. 3. Boston: Springer. https://doi.org/10.1007/978-0-387-78151-8_48
- Heppell, S.S., Caswell, H. & Crowder, L.B. (2000). Life histories and elasticity patterns: perturbation analysis for species with minimal demographic data. *Ecology* **81**, 654–665.
- Himes Boor, G.K., McGuire, T.L., Warlick, A.J., Taylor, R.L., Converse, S.J., McClung, J.R. & Stephens, A.D. (2023). Estimating reproductive rates and juvenile survival when offspring ages are uncertain using a novel multievent mark-recapture model. *Methods Ecol. Evol.* **14**, 631–642.
- Hobbs, R.C., Shelden, K.E.W., Vos, D.J., Goetz, K.T. & Rugh, D.J. (2006). *Status review and extinction assessment of Cook Inlet belugas (Delphinapterus leucas)*. AFSC Processed Rep. 2006-16, 74 p. <https://repository.library.noaa.gov/view/noaa/8592>
- Hobbs, R.C., Wade, P.R. & Shelden, K.E.W. (2015). Viability of a small, geographically-isolated population of beluga whale, *Delphinapterus leucas*: effects of hunting, predation, and mortality events in Cook Inlet, Alaska. *Mar. Fish. Rev.* **77**, 59–88.
- Jacobson, E.K., Boyd, C., McGuire, T.L., Shelden, K.E.W., Himes-Boor, G.K.H. & Punt, A.E. (2020). Assessing cetacean populations using integrated population models: an example with Cook Inlet beluga whales. *Ecol. Appl.* **30**, e02114.
- Jenouvrier, S., Holland, M., Iles, D., Labrousse, S., Landrum, L., Garnier, J., Caswell, H., Weimerskirch, H., LaRue, M., Ji, R. & Barbraud, C. (2020). The Paris Agreement objectives will likely halt future declines of emperor penguins. *Glob. Chang. Biol.* **26**, 1170–1184.
- Jones, L.A., Schoen, E.R., Shaftel, R., Cunningham, C.J., Mauger, S., Rinella, D.J. & St. Saviour, A. (2020). Watershed-scale climate influences productivity of Chinook salmon populations across southcentral Alaska. *Glob. Chang. Biol.* **26**, 4919–4936.
- Jordaan, R.K., Oosthuizen, W.C., Reisinger, R.R. & Bruyn, P.J.N.D. (2020). Abundance, survival and population growth of killer whales *Orcinus orca* at subantarctic Marion Island. *Wildl. Biol.* **2020**, wlb.00732.
- Kellner, K. (2019). A wrapper around ‘rjags’ to streamline ‘JAGS’ analyses, jagsUI v1.5.1. <https://github.com/kenkellner/jagsUI/releases>
- Kéry, M. & Schaub, M. (2012). *Bayesian population analysis using WinBUGS*. Waltham, MA: Elsevier.
- Lacy, R.C., Williams, R., Ashe, E., Balcomb, K.C., III, Brent, L.J.N., Clark, C.W., Croft, D.P., Giles, D.A., MacDuffee, M. & Paquet, P.C. (2017). Evaluating anthropogenic threats to endangered killer whales to inform effective recovery plans. *Sci. Rep.* **7**, 14119.
- Lande, R. (1988). Genetics and demography in biological conservation. *Science* **241**, 1455–1460.
- Lawler, J.J., Campbell, S.P., Guerry, A.D., Kolozsvary, M.B., O'Connor, R.J. & Seward, L.C.N. (2002). The scope and treatment of threats in endangered species recovery plans. *Ecol. Appl.* **12**, 663–667.
- Lesage, V. (2021). The challenges of a small population exposed to multiple anthropogenic stressors and a changing climate: the St. Lawrence Estuary beluga. *Polar Res.* **40**, 5523.
- Litzow, M.A., Ciannelli, L., Puerta, P., Wettstein, J.J., Rykaczewski, R.R. & Opiekun, M. (2018). Non-stationary climate–salmon relationships in the Gulf of Alaska. *Proc. Biol. Sci.* **285**, 20181855. <https://doi.org/10.1098/rspb.2018.1855>
- Luque, S.P. & Ferguson, S.H. (2010). Age structure, growth, mortality, and density of belugas (*Delphinapterus leucas*) in the Canadian Arctic: responses to environment? *Polar Biol.* **33**, 163–178.
- Manlik, O., McDonald, J.A., Mann, J., Raudino, H.C., Bejder, L., Krützen, M., Connor, R.C., Heithaus, M.R., Lacy, R.C. & Sherwin, W.B. (2016). The relative importance of reproduction and survival for the conservation of two dolphin populations. *Ecol. Evol.* **6**, 3496–3512.
- McGuire, T.L., Stephens, A.D., McClung, J.R., Garner, C.D., Shelden, K.E.W., Himes Boor, G.K. & Wright, B. (2020). Reproductive natural history of endangered Cook Inlet beluga whales: insights from a long-term photo-identification study. *Polar Biol.* **43**, 1851–1871.
- Moore, S.E. (2018). Climate change. In *The encyclopedia of marine mammals*: 194–197. Würsig, B., Thewissen, J.G.M. & Kovacs, K.M. (Eds). 3rd edn. San Diego, CA: Academic Press/Elsevier.
- Moore, S.E., Shelden, K.E.W., Rugh, D.J., Mahoney, B.A. & Litzky, L.K. (2000). Beluga whale habitat associations in Cook Inlet, Alaska. *Mar. Fish. Rev.* **62**, 60–80.
- Mosnier, A., Doniol-Valcroze, T., Gosselin, J.-F., Lesage, V., Measures, L.N. & Hammill, M.O. (2015). Insights into processes of population decline using an integrated population model: the case of the St. Lawrence Estuary beluga (*Delphinapterus leucas*). *Ecol. Model.* **314**, 15–31.
- National Marine Fisheries Service (NMFS). (2016). *Recovery plan for the Cook Inlet beluga whale (Delphinapterus leucas)*. Juneau, AK: National Marine Fisheries Service, Alaska Region, Protected Resources Division. <https://repository.library.noaa.gov/view/noaa/15979>
- Nelson, M., Quakenbush, L., Mahoney, B., Taras, B. & Wooller, M. (2018). Fifty years of Cook Inlet beluga whale feeding ecology from isotopes in bone and teeth. *Endang. Species Res.* **36**, 77–87.

- O'Neill, S.M., Ylitalo, G.M. & West, J.E. (2014). Energy content of Pacific salmon as prey of northern and southern resident killer whales. *Endang. Species Res.* **25**, 265–281.
- Pirotta, E., Thomas, L., Costa, D.P., Hall, A.J., Harris, C.M., Harwood, J., Kraus, S.D., Miller, P.J.O., Moore, M.J., Photopoulou, T., Rolland, R.M., Schwacke, L., Simmons, S.E., Southall, B.L. & Tyack, P.L. (2022). Understanding the combined effects of multiple stressors: a new perspective on a longstanding challenge. *Sci. Total Environ.* **821**, 153322.
- Plummer, M. (2019). rjags: bayesian graphical models using MCMC. R package version 4-10. <https://CRAN.R-project.org/package=rjags>
- Pradel, R., Gimenez, O. & Lebreton, J. (2005). Principles and interest of GOF tests for multistate capture–recapture models. *Anim. Biodivers. Conserv.* **28**, 189–204.
- Quakenbush, L.T., Suydam, R.S., Brown, A.L., Lowry, L.F., Frost, K.J. & Mahoney, B.A. (2015). Diet of beluga whales, *Delphinapterus leucas*, in Alaska from stomach contents, March–November. *Mar. Fish. Rev.* **77**, 70–84.
- R Core Development Team. (2022). *R: a language and environment for statistical computing*. Vienna: R Foundation for Statistical Computing. <https://www.R-project.org/>
- Regehr, E.V., Hostetter, N.J., Wilson, R.R., Rode, K.D., Martin, M.S. & Converse, S.J. (2018). Integrated population modeling provides the first empirical estimates of vital rates and abundance for polar bears in the Chukchi Sea. *Sci. Rep.* **8**, 16780.
- Rhodes, J.R., Ng, C.F., de Villiers, D.I., Preece, H.J., McAlpine, C.A. & Possingham, H.P. (2011). Using integrated population modelling to quantify the implications of multiple threatening processes for a rapidly declining population. *Biol. Conserv.* **144**, 1081–1088.
- Runge, M.C., Langtimm, C.A. & Kendall, W.L. (2004). A stage-based model of manatee population dynamics. *Mar. Mamm. Sci.* **20**, 361–385.
- Saunders, S.P., Cuthbert, F.J. & Zipkin, E.F. (2018). Evaluating population viability and efficacy of conservation management using integrated population models. *J. Appl. Ecol.* **55**, 1380–1392.
- Shelden, K.E.W., Burns, J.J., McGuire, T.L., Burek-Huntington, K.A., Vos, D.J., Goertz, C.E.C., O'Corry-Crowe, G. & Mahoney, B.A. (2020). Reproductive status of female beluga whales from the endangered Cook Inlet population. *Mar. Mamm. Sci.* **36**, 690–699.
- Shelden, K.E.W., Goetz, K.T., Rugh, D.J., Calkins, D.G., Mahoney, B.A. & Hobbs, R.C. (2015). Spatio-temporal changes in beluga whale, *Delphinapterus leucas*, distribution: results from aerial surveys (1977–2014), opportunistic sightings (1975–2014), and satellite tagging (1999–2003) in Cook Inlet, Alaska. *Mar. Fish. Rev.* **77**, 1–31.
- Shelden, K.E.W. and P.R. Wade. 2019. Aerial surveys, distribution, abundance, and trend of belugas (*Delphinapterus leucas*) in Cook Inlet, Alaska, June 2018. AFSC Processed Report 2019-09, 93 p. <https://doi.org/10.25923/kay8-7p06>
- Simons, R.A. (2019). *ERDDAP*. Monterey, CA: NOAA/NMFS/SWFSC/ERD. <https://coastwatch.pfeg.noaa.gov/erddap>
- Simpson, D., Rue, H., Riebler, A., Martins, T.G. & Sørbye, S.H. (2017). Penalising model component complexity: a principled, practical approach to constructing priors. *Statist. Sci.* **32**, 1–28.
- Taylor, B.L., Martinez, M., Gerrodette, T., Barlow, J. & Hrovat, Y.N. (2007). Lessons from monitoring trends in abundance of marine mammals. *Mar. Mamm. Sci.* **23**, 157–175.
- Warlick, A.J., Himes Boor, G.K., McGuire, T.L., Shelden, K.E.W., Jacobson, E.K., Boyd, C., Wade, P.R., Punt, A.E. & Converse, S.J. (2023). Github repository: quantitative-Conservation-Lab/Warlick_etal_2023_AnimalConservation. <https://doi.org/10.5281/zenodo.8212991>
- Watanabe, S. (2010). Asymptotic equivalence of Bayes cross validation and widely applicable information criterion in singular learning theory. *J. Mach. Learn. Res.* **11**, 3571–3594.
- White, G.C. (2000). Population viability analysis: data requirements and essential analyses. In *Research techniques in animal ecology: controversies and consequences*: 288–331. Boitani, L. & Fuller, T.K. (Eds). New York, New York: Columbia University Press.
- Williams, P.J., Hooten, M.B., Womble, J.N., Esslinger, G.G., Bower, M.R. & Hefley, T.J. (2017). An integrated data model to estimate spatiotemporal occupancy, abundance, and colonization dynamics. *Ecology* **98**, 328–336.
- Zipkin, E.F. & Saunders, S.P. (2018). Synthesizing multiple data types for biological conservation using integrated population models. *Biol. Conserv.* **217**, 240–250.

Supporting information

Additional supporting information may be found online in the Supporting Information section at the end of the article.

Appendix S1. Sensitivity of demography, abundance, and viability to underlying assumptions of the aerial survey model in an IPM-based PVA for Cook Inlet belugas.

Appendix S2. Sensitivity of demography, abundance, and viability to age at first birth for Cook Inlet beluga whales.

Appendix S3. Expanded covariate analysis for Cook Inlet belugas.

Appendix S4. Defining a quasi-extinction threshold for Cook Inlet belugas.

Appendix S5. Detailed ecological and observation process model results and sensitivity analysis for Cook Inlet belugas.